Continuous Alloy-Composition Spatial Grading and Superbroad Wavelength-Tunable Nanowire Lasers on a Single Chip

ARTICLE *in* NANO LETTERS · FEBRUARY 2009

Impact Factor: 13.59 · DOI: 10.1021/nl803456k · Source: PubMed

NANO LETTERS

2009
Vol. 9, No. 2
784-788

Continuous Alloy-Composition Spatial Grading and Superbroad Wavelength-Tunable Nanowire Lasers on a Single Chip

Anlian Pan,[†] Weichang Zhou,[†,‡] Eunice S. P. Leong,[†] Ruibin Liu,[†] Alan H. Chin,[†] Bingsuo Zou,[‡,§] and C. Z. Ning*[,†]

Department of Electrical Engineering and Center for Nanophotonics, Arizona Institute of NanoElectronics, Arizona State University, Tempe, Arizona 85287, Key Laboratory for Micro-Nano Optoelectronic Devices of Ministry of Education and Micro-Nanotechnology Research Center, Hunan University, Changsha, 410082, China and School of MSE, Beijing Institute of Technology, Beijing 100081, China

Received November 14, 2008

ABSTRACT

By controlling local substrate temperature in a chemical vapor deposition system, we have successfully achieved spatial composition grading covering the complete composition range of ternary alloy CdSSe nanowires on a single substrate of 1.2 cm in length. Spatial photoluminescence scan along the substrate length shows peak wavelength changes continuously from ~500 to ~700 nm. Furthermore, we show that under strong optical pumping, every spot along the substrate length displays lasing behavior. Thus our nanowire chip provides a spatially continuously tunable laser with a superbroad wavelength tuning range, unmatched by any other available semiconductor-based technology.

Wavelength flexibility, variety, and controllability are important for almost any application of lasers, but producing lasers with large wavelength-tunability is fundamentally difficult in a conventional approach based on planar growth technology due to lattice mismatch. A few discrete lasing wavelengths can be achieved through multiple electronic transitions in gas or solution phase molecular materials, doped solid state materials, or more recently in quantum well based intersubband lasers with three discrete lasing wavelengths.[1] An ultimate wavelength-flexible laser would ideally be able to tune to any wavelength in a controllable fashion over a wide wavelength range on a single semiconductor chip. Since the wavelength of a semiconductor laser is determined by its fundamental band gap, such semiconductor lasers would require band-gap-tunable alloy semiconductors with composition variation in a large range on a single chip. Alloying semiconductors of different band gaps has long been one of the standard methods of achieving new band gaps (and thus the operating wavelength of an optical device) that are not provided by naturally occurring semiconductors. Unfortunately, this method of achieving wavelength variability is severely limited in the existing methods of growing planar epitaxial heterostructures of semiconductor thin films on a crystalline substrate, since a close match of lattice constants of the substrate and the alloy materials to be grown (or a means of relieving the strain due to lattice mismatch) is required. The very limited lattice-constant mismatch required for growing high-quality wafers has been the main obstacle of making semiconductor-based optoelectronic devices (such as lasers, detectors, and solar cells) with controllable and widely variable operating wavelengths. With the advent of nanowire-based technology, such restrictions are removed or are very much relaxed, depending on the method of growth. For epitaxial growth of nanowires, the relaxed requirement of lattice matching has led to the growth of materials with a mismatch as large as 8%.[2] InP, GaAs, and other III−V nanowires have been epitaxially grown on Si[2], and InAs and InP nanowires have been grown into nanowire heterostructures,[3] despite large lattice mismatches. In addition, nanowires can also be grown using an amorphous substrate as simply a mechanical support, allowing alloy nanowire growth with a much larger range of composition variation than is possible with planar growth technologies. This has led to the growth of a wide range of alloy

* Corresponding author, cning@asu.edu.
[†] Department of Electrical Engineering and Center for Nanophotonics, Arizona Institute of NanoElectronics, Arizona State University.
[‡] Key Laboratory for Micro-Nano Optoelectronic Devices of Ministry of Education and Micro-Nanotechnology Research Center, Hunan University.
[§] School of MSE, Beijing Institute of Technology.

10.1021/nl803456k CCC: $40.75
Published on Web 01/27/2009

compositions between two binary compounds such as CdS and CdSe,[4,5] InN and GaN,[6] ZnS and CdS,[7] ZnSe and CdSe,[8] ZnO and MgO,[9] and so on. Such alloy composition variation provides unprecedented access to new wavelength ranges using semiconductor alloys. In this connection, it is worth mentioning that semiconductor nanoparticle (nanocrystal) technology can also provide a large range of wavelength flexibility by either alloying or size variation. But for optical applications, nanowire alloys have an additional advantage not available with nanoparticles, since individual nanowires intrinsically provide both channels for electronic conduction, and waveguides for optical devices, in addition to serving as a gain material. This is why individual nanowires have been shown to act as nanolasers.[10−17]

Although various semiconductor alloy nanowires or nanobelts of different compositions have been achieved under *separate* growth conditions, it is both challenging and important to achieve a full-range composition variation within a *single* substrate in a *single* run of growth. To achieve fully tunable *lasing* within the entire composition range on a single substrate would be even more appealing and challenging. Demonstration of $In_xGa_{1-x}N$ nanowires over the entire composition range was reported recently.[6] Alloy composition dependent lasing was demonstrated between 365 and 494 nm using InGaN/GaN multiple quantum well nanowires.[18] All these demonstrate the great potential and power of a nanowire-based approach in achieving widely tunable light emission through alloy composition control. Here we demonstrate a different (and complementary) approach using a carefully designed longitudinal temperature gradient along the tube direction. Our results demonstrate that CdSSe alloy nanowires of very high aspect ratio can be grown with composition grading along the substrate length direction, so that the complete alloy composition between the two binaries is covered in a substrate of ∼1.2 cm in length. We also demonstrate that such nanowires at their native substrate function as spatially wavelength-tunable lasers at high optical pumping, providing the first example of a continuously tunable laser with an unprecedented tuning range of over 200 nm. Such broadly tunable lasers may find use in many applications such as novel optical interconnects or multiplexing, multiagent chemical or biological detections, solid-state lighting, solar cells, and superbright microdisplays, among many others.

To demonstrate such wide spatially tunable lasing, we chose the ternary alloy CdS_xSe_{1-x} (CdSSe) in the full composition range between CdS ($x = 1$, band gap 2.44 eV) and CdSe ($x = 0$, band gap 1.72 eV), because they are two important compound semiconductors that are of great interest for their emission in the visible wavelength range and have been investigated for their one-dimensional nanostructures and alloys recently.[4,5,13,19−21] For example, CdSSe alloy nanobelts with several compositions were grown by changing the ratio of the source powders (CdS and CdSe) and/or the growth temperature of the substrate.[4,5] To grow CdSSe nanowires in the full range of alloy composition on a single substrate in a single run of growth, comprehensive optimization involving substrate locations, flux rates of semiconductor vapors, and, most importantly, control of the temperature

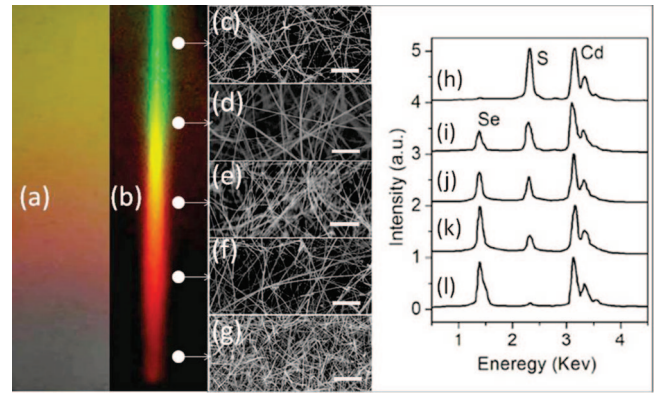

Figure 1. The real-color photographs of a quartz substrate with the as-grown spatially composition-graded CdSSe nanowires under room lighting (a) and under UV laser illumination (b) (266 nm). Size of the substrate: 0.3 × 1.2 cm. (c−g) The SEM images taken at the white spots in panel b, respectively. Scale bar: 5 μm. (h−l) The in situ EDS corresponding to the five SEM images.

gradient are necessary. More specifically, for a given combination of flux rates and location and length of the substrate, a large enough temperature gradient is required and the range of temperatures on the substrate must be appropriate to grow the full alloy composition range of CdSSe nanowires simultaneously in a spatially correlated fashion. For this purpose, we have specially designed a short tube furnace with a very short central heating zone and with the ends of the furnace equipped with an efficient cooling mechanism during the growth of sample. With this setup, we could achieve a very large temperature gradient in a short spatial interval of ∼1.2 cm along the tube axis with a temperature variation between ∼580 and ∼690 °C, as shown in Figure S1 (Supporting Information). This temperature range covers the full temperature range required to grow the complete composition range of CdSSe in a single run of growth (see the Supporting Information for the growth details).

Panels a and b of Figure 1 show the real-color photographs of a quartz substrate with the as-grown nanowires under regular room lighting (a) and under a UV laser (266 nm) illumination (b) (see the Supporting Information for this experiment), respectively. The as-grown sample shows the color change gradually from light-yellow (as seen in the CdS source powder) to dark (as seen in the CdSe source powder) along the sample length direction, while the photoluminescence (PL) photograph exhibits the color change from green (consistent to the PL color of CdS) to red (consistent to the PL color of CdSe) along the same direction. These results indicate the formation of composition graded CdSSe alloys on a single substrate. Panels c−g of Figure 1 are five scanning electron microscopy (SEM) images taken from selected spots along the sample length as indicated by the white spots in Figure 1b, respectively. The SEM results show that the whole substrate is covered with nanowires, with their diameter around 200 nm and length up to several tens of micrometers. Curves h−l in Figure 1 show the in situ energy dispersive X-ray spectra (EDS) at the same locations where the five SEM images in Figure 1c−g were taken, respectively (see the Supporting Information for the SEM and EDS experiment details). The EDS result indicates that all the

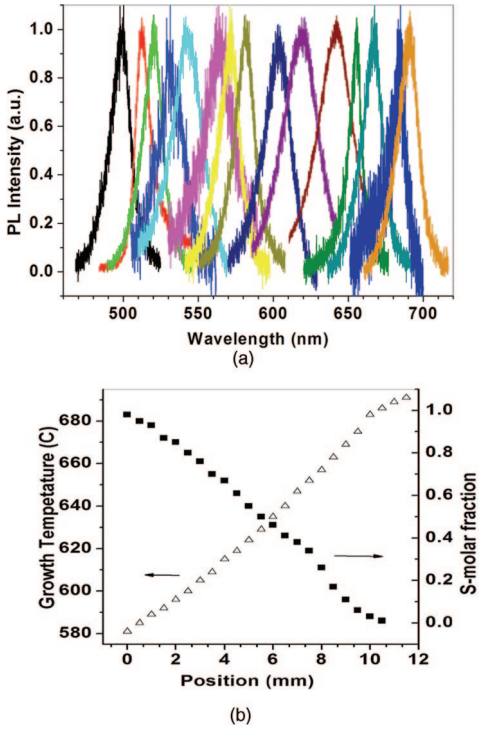

Figure 2. (a) Micro-PL spectra collected at different locations along the substrate length at cryostat temperature of 77 K. (b) Substrate temperature (left coordinate) and S-molar fraction (right coordinate, extracted from the EDS measurement shown in Figure 2) measured at different points along the substrate length.

nanowires along the substrate are composed of Cd, S, and Se, and the Se-fraction is complementary to that of S, which gives direct evidence that the obtained sample is the spatially composition-graded CdSSe nanowires along the length direction.

Figure 2a shows the representative PL spectra at $T = 77$ K of spatially composition-graded CdSSe nanowires (see the Supporting Information for the PL experiments). The micro-PL spectra taken at 15 different points along the length of the substrate show no midgap emission band, indicating high-quality single crystal nanowires with negligible surface states, consistent with the TEM (not shown) and the X-ray diffraction (XRD, see Figure S2 in the Supporting Information) measurements. The PL peaks vary between 498 and 692 nm, covering a large part of the visible spectrum. To associate different PL peaks at different locations of the substrate to the growth temperature and the local alloy composition, we plot in Figure 2b the measured substrate temperature and the S-molar fraction extracted from a more refined spatial-resolved EDS measurements. A more refined spatial-resolved measurement of the PL peaks is shown in Figure 3a. Knowing the spatial dependence of the alloy composition through EDS and that of the PL wavelength at the same time, we can readily relate the alloy composition to the PL peak directly. In Figure 3b, we plot the PL peak as a function of the S-molar fraction (filled squares). Furthermore, it is known that the band gap of a ternary alloy is determined by an interpolation between those of the two binaries with additional nonlinear bowing

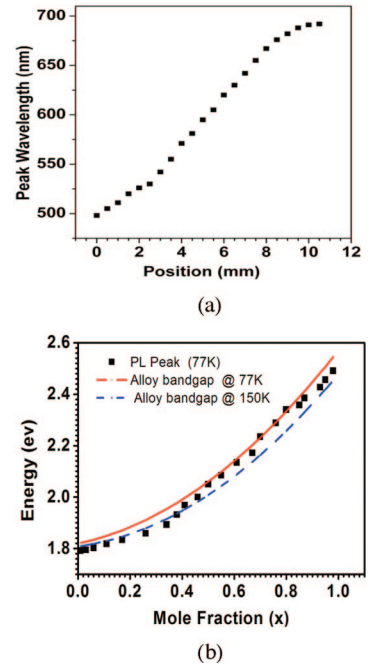

Figure 3. (a) PL peak wavelengths as a function of substrate length coordinate. (b) Band gap of the alloy (lines) obtained from eq 1 and PL peak energy (squares) as a function of alloy composition determined from the EDS data shown in Figure 3b.

$$E_g(AB_xC_{1-x}) = xE_g(AB) + (1-x)E(AC) - x(1-x)b \quad (1)$$

For $CdSe_xS_{1-x}$ the band gap bowing parameter $b = 0.54$ according to ref 22. Using the alloy composition determined by EDS as shown in Figure 2b, we can obtain band gap for each molar fraction by using eq 1. The resulting band gap dependence on composition at $T = 77$ K is plotted as a solid line in Figure 3b. We see that there is a good overall agreement between the PL peak energy and the band gap at each given molar fraction. To get an idea of the possible laser-induced temperature rise, we also plotted the band gap at a higher temperature ($T = 150$ K, as represented by the dashed line), which is apparently higher than the actual temperature of nanowires. Therefore the actual sample temperature is somewhere between 77 and 150 K due to laser-induced heating. From this comparison, it is clear that we have achieved a quasi-continuous change of alloy compositions by using the temperature gradient and that such continuous alloy grading leads to a spatial grading of the wavelength of emitted light over a wide wavelength range.

To demonstrate the possibility of widely tunable *lasing*, we performed similar micro-PL measurements to that described above, but with increased laser-excitation intensity. Figure 4 shows results of this experiment where PL spectra from 16 spots were taken along the length of the substrate maintained at 77 K. We see that extremely sharp lines now emerge from the broad spontaneous emission background at every spot. Compared to the PL spectra shown in Figure 2a, we see clearly lasing has occurred at each point with some of the spots showing multimode lasing. The mechanism of lasing is similar to what has been reported widely in semiconductor nanowires where individual wires can act as laser cavities[11,12,15−17] with two ends providing feedback. The lasing wavelength range is measured from 503 to 692 nm. We emphasize that this is the *first* demonstration of spatially

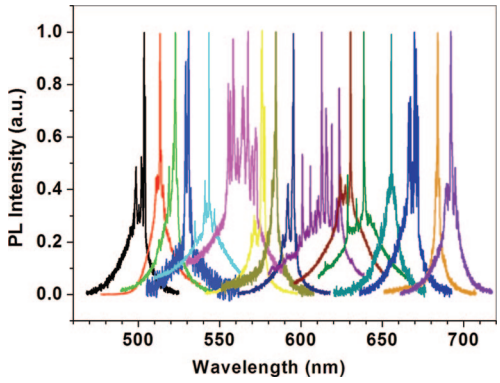

Figure 4. Micro-PL collected at various locations along the substrate maintained at 77 K under high optical pumping condition showing lasing or multimode lasing.

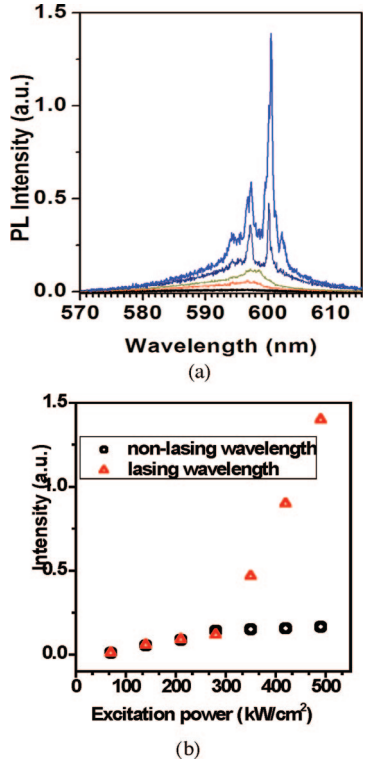

Figure 5. (a) Evolution of the PL spectrum from spontaneous emission to lasing as pumping is increased. (b) PL intensity at lasing wavelength (triangles) and at a nonlasing wavelength of 592 nm (circles).

tunable semiconductor nanowire lasers with wide-wavelength coverage, to the best of our knowledge. The wavelength coverage of $\Delta\lambda = 189$ nm is the widest ever reported for any semiconductor material. Achieving this relative tunability of $\Delta\lambda/\lambda = 32\%$ on a single as-grown substrate of $\sim$1.2 cm is even more remarkable.

Figure 5a shows a sequence of PL spectra collected at a given spot with increasing pump intensity levels to show the detailed transition process from spontaneous emission to lasing. We again see a clear transition from broadband emission to sharp lasing peaks. The multiple peaks could be either from multiple modes of a single nanowire or from different nanowires with different lengths. To see the same laser transition from a different perspective, we plot in Figure 5b the light intensity collected at two fixed wavelengths as a function of pumping intensity. One wavelength is where laser peak eventually appears, showing a transition from spontaneous emission to lasing, and the other wavelength (592 nm) is outside of the peak region, reflecting how spontaneous emission changes with pumping around the laser threshold. As expected of a typical laser threshold, spontaneous emission starts to saturate at a pumping level where lasing wavelength shows a clear transition. After the transition, the spontaneous emission maintains at a saturated level, with slight increase due to laser-induced heating by the excitation laser, while the lasing mode increases its intensity linearly with the intensity of the excitation laser. Notice that there is a broad spectral background in most of the lasing spectra. We believe that most of the background is from the spontaneous emission from the neighboring nonlasing wires. This is very often the case for the wires on the original substrates where wire density is relatively high. The nonlasing wires eventually heat up the samples and prevent lasing at high temperature. To illustrate this point, we remove the wires from the original substrate and disperse onto another substrate such that there are no other wires in the neighborhood of a given wire within the excitation spot, so that lasing from individual wires can be studied. This is shown in Figure S3 (see the Supporting Information) where lasing spectra at increasing pump levels are shown in Figure S3a and the line width as a function of the pumping level is shown in Figure S3b. As one can see from Figure S3a, the spectral feature shows a largely saturated spontaneous emission background. The line width shows a typical dramatic reduction at the threshold. The combination of the spectra and the line width shows a convincing laser threshold behavior. Interestingly, this measurement was performed at room temperature, while most of the nanowires on the original substrate typically do not show lasing at room temperature. This demonstrates the high quality of nanowires and simultaneously indicates that the main reason that we could not obtain room temperature lasing on the as-grown substrate is the high density of the wires and the emission/absorption of nonlasing nearby nanowires.

In summary, we have demonstrated an unprecedented semiconductor laser chip with the widest wavelength tuning range ever, continuously tunable over the length of the chip. Such a multiwavelength laser chip can be used for a wide variety of applications, such as an on-chip wavelength division multiplexing (WDM) source, a multiwavelength sensor, an optimizable white-light source, red−green−blue (RGB) display, and nanophotonics integrated circuits. The unique widely band-gap-graded nanomaterials can also be of great potential use as a material base for full-spectral-coverage solar cells or for a spectrometer on-a-chip. The results reported here open the way for many exciting applications of this new class of nanomaterials.

Acknowledgment. The ASU team thanks Science Foundation of Arizona (SFAz) and the US Army Research Office for financial support. The Hunan University team thanks the NSF (term no. 90606001 and 50602015) of China and the

Hunan Provincial Natural Science Foundation of China (Distinguished Young Scholars) for financial support.

Supporting Information Available: Experiment details for sample growth, XRD, SEM, and EDS characterizations, and PL measurements, temperature profile along the reactor length, lasing spectra and line width at room temperature from a dispersed wire. This material is available free of charge via the Internet at http://pubs.acs.org.

References

(1) Tredicucci, A.; Gmachl, C.; Capasso, F.; Sivco, D. L.; Hutchinson, A. L.; Cho, A. Y. *Nature* **1998**, *396*, 350.

(2) Martensson, T.; Patrik, C.; Wacaser, B.; Larsson, M.; Seifert, W.; Deppert, K.; Gustafsson, A.; Wallenberg, L.; Samuelson, L. *Nano Lett.* **2004**, *4*, 1987.

(3) Bjork, M.; Ohlsson, B.; Sass, T.; Persson, A.; Thelander, C.; Magnusson, M.; Deppert, K.; Wallenberg, L.; Samuelson, L. *Nano Lett.* **2002**, *2*, 87.

(4) Pan, A. L.; Yang, H.; Liu, R. B.; Yu, R. C.; Zou, B. S.; Wang, Z. L. *J. Am. Chem. Soc.* **2005**, *127*, 15692.

(5) Pan, A. L.; Yang, H.; Yu, R. C.; Zou, B. S. *Nanotechnology* **2006**, *17*, 1083.

(6) Kuykendall, T.; Ulrich, P.; Aloni, S.; Yang, P. D. *Nat. Mater.* **2007**, *6*, 951.

(7) Liu, Y.; Zapien, J. A.; Shan, Y. Y.; Geng, C. Y.; Lee, C. S.; Lee, S. T. *Adv. Mater.* **2005**, *17*, 1372.

(8) Shan, C. X.; Liu, Z.; Ng, C. M.; Hark, S. K. *Appl. Phys. Lett.* **2005**, *87*, 033108.

(9) Lu, G. Y.; Zhang, Y. Z.; Ye, Z. Z.; Zeng, Y. J.; Huang, J. Y.; Wang, L. *Appl. Phys. Lett.* **2007**, *91*, 193108.

(10) Huang, M. H.; Mao, S.; Feick, H.; Yan, H.; Wu, Y.; Kind, H.; Weber, E.; Russo, R.; Yang, P. D. *Science* **2001**, *292*, 1897.

(11) Johnson, J. C.; Yan, H. Q.; Schaller, R. D.; Haber, L. H.; Saykally, R. J.; Yang, P. D. *J. Phys. Chem. B* **2001**, *105*, 11387.

(12) Duan, X.; Huang, Y.; Agarwal, R.; Lieber, C. M. *Nature* **2003**, *421*, 241.

(13) Agarwal, R.; Barrelet, C.; Lieber, C. M. *Nano Lett.* **2005**, *5*, 917.

(14) Zapien, J. A.; Jiang, Y.; Meng, X.; Chen, W.; Au, F.; Lifshitz, Y.; Lee, S. T. *Appl. Phys. Lett.* **2004**, *84*, 1189.

(15) Chin, A. H.; Vaddiraju, S.; Maslov, A. V.; Ning, C. Z.; Sunkara, M. K.; Meyyappan, M. *Appl. Phys. Lett.* **2006**, *88*, 163115.

(16) Maslov, A. V.; Ning, C. Z. *Appl. Phys. Lett.* **2003**, *83*, 1237.

(17) Maslov, A. V.; Ning, C. Z. *IEEE J. Quantum Electron.* **2004**, *40*, 1389.

(18) Qian, F.; Li, Y.; Gradecak, S.; Park, H.; Dong, Y.; Ding, Y.; Wang, Z. L.; Lieber, C. M. *Nat. Mater.* **2008**, *7*, 701.

(19) Yu, H.; Li, J.; Loomis, R. A.; Gibbons, P. C.; Wang, L. W.; Buhro, W. E. *J. Am. Chem. Soc.* **2003**, *125*, 16168.

(20) Barrelet, C. J.; Greytak, A. B.; Lieber, C. M. *Nano Lett.* **2004**, *4*, 1981.

(21) Ma, R.; Dai, L.; Huo, H.; Xu, W.; Qin, G. G. *Nano Lett.* **2007**, *7*, 3300.

(22) Hill, R. *J. Phys. C: Solid State Phys.* **1974**, *7*, 521.

NL803456K